Observed and Modeled Wind and Water-Level Response from Tropical Storm Marco (1990)

SAM H. HOUSTON AND MARK D. POWELL

AOML/NOAA, Hurricane Research Division, Miami, Florida

(Manuscript received 26 August 1993, in final form 30 March 1994)

ABSTRACT

The Hurricane Research Division (HRD) analyzes surface wind fields in tropical storms and hurricanes using surface wind observations and aircraft flight-level wind measurements in the vicinity of the storms. The analyzed surface wind fields for Tropical Storm Marco (1990) were compared with the wind fields used for input in the National Weather Service's Sea, Lake, and Overland Surge from Hurricanes (SLOSH) model. The HRD wind fields were also used to determine the wind speeds and directions corresponding to the storm surge at tide gauges along Florida's west coast. The observed storm surge at the gauges was compared with the storm surge computed by the SLOSH model. Time series of the SLOSH model winds were compared with time series based on the analyzed wind field at each tide gauge, because in most cases there were no wind observations available at these gauges. The comparisons of the analyzed and modeled winds and the observed and modeled storm surge show that the SLOSH model reasonably represented the extreme storm tide effects on two basins with relatively complicated coastlines. However, SLOSH overestimated surface winds in areas of offshore flow, resulting in predictions of excessive negative surge. It is suggested that real-time storm surge model calculations, based on input from real-time surface wind analyses, have potential for the support of emergency management response and infrastructure recovery efforts during and immediately following landfall.

1. Introduction

In recent years the hurricane warning system has improved (e.g., McAdie and Lawrence 1993), but due to the increased coastal population, the amount of time has increased for the safe evacuation of people from barrier islands and other vulnerable coastal areas (Sheets 1990). In a few critical locations, the roadway systems are incapable of evacuating the population in less than the lead time of National Weather Service (NWS) warnings. This problem is exacerbated, according to Jarrell et al. (1992), because 80%–90% of the people who live in hurricane-prone areas have never experienced the core of a major hurricane of category 3 or higher on the Saffir–Simpson hurricane scale (Saffir 1977). Even relatively weak tropical storms can produce winds and storm surges that isolate low-lying coastal areas. A case in point was Tropical Storm (TS) Marco, the only tropical cyclone that crossed the coastline of the United States during 1990. Marco struck Florida's Tampa Bay area, a region especially susceptible to storm surge (no evacuation routes were reported closed due to the storm surge during Marco) on 11 October (Fig. 1).

Corresponding author address: Sam H. Houston, NOAA/ERL, Hurricane Research Division/AOML, 4301 Rickenbacker Causeway, Miami, FL 33149-1097.

a. The SLOSH model and evacuation planning

Tropical Storm Marco illustrates many of the storm surge forecast problems that occur during the landfall of a weak storm along a heavily populated coastline. The main forecast guidance for storm surge in tropical storms and hurricanes is the Sea, Lake, and Overland Surge from Hurricanes (SLOSH) model (Jelesnianski et al. 1992). Although Jelesnianski et al. (1992) describe the SLOSH model as a real-time forecast model, in its present form it is not possible to run the model with forcing from objectively analyzed wind fields in real time. The SLOSH model water levels are forced by an idealized wind field that depends upon the pressure deficit (Δp) and the radius of the maximum wind (R_{MW}) from the storm center. In its calculations of water levels, the model incorporates topography, channels, barriers, etc., but does not include astronomical tides, waves, or flooding from rainfall. Comparisons of observed and SLOSH-computed storm surge have been conducted by Jarvinen and Lawrence (1985) for 10 hurricanes and by Jarvinen and Gebert (1986, 1987) and Jarvinen and McDuffie (1987) for Hurricane Gloria (1985). Validation studies have not related observed and model-calculated storm surge to time-dependent forcing by analyzing the surface wind. However, there have been comparisons of SLOSH model–calculated winds in a few cases where wind observations were located in the vicinity of tide gauges (Jelesnianski et al. 1992). Model performance in trop-

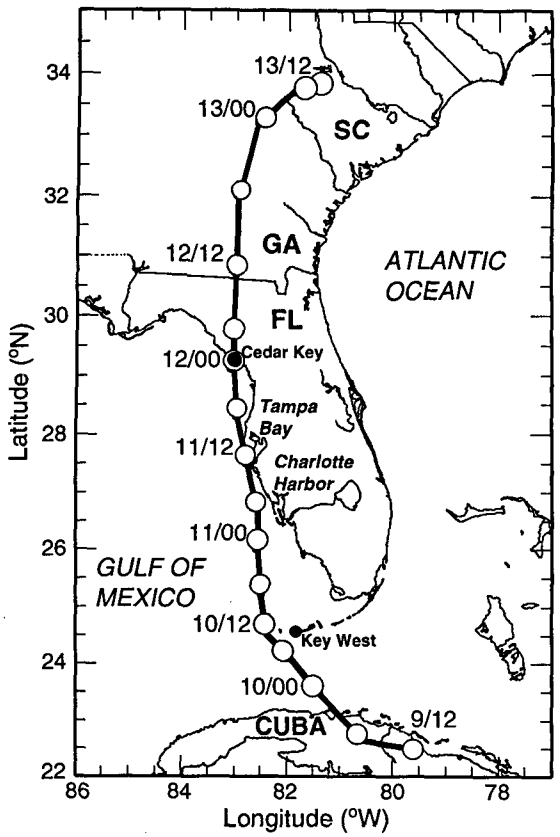

FIG. 1. Best-track positions for TS Marco every 6 h; the date and hour (UTC) are shown every 12 h.

ical cyclones of tropical storm strength has not been documented.

As part of comprehensive hurricane evacuation studies funded by the Federal Emergency Management Agency, the SLOSH model is used to map the storm surge flood plain in each of the coastal SLOSH basins. The characteristics of each of these basins, such as topography and other hydrodynamic parameters, are based on data gathered by government agencies like the National Oceanic and Atmospheric Administration's (NOAA's) National Ocean Service (NOS) and the U.S. Geological Survey (USGS). An atlas is produced for each SLOSH basin, based on hypothetical hurricanes along various tracks, with different speeds and strengths. This atlas provides general guidance for emergency preparation and evacuation.

b. Real-time applications for storm surge modeling

Evacuation lead times for many urban areas are in excess of 24 h; track and intensity forecast uncertainty (Sheets 1990) at these timescales is such that little is gained by attempting storm surge forecasts in an operational mode. In the 0–6-h time frame, however, the SLOSH model can be run in real time to assess the effectiveness and extent of the warnings. During and after landfall, SLOSH calculations could provide an immediate assessment of the extent of storm surge inundation. In major storms, this information is critical to emergency managers for effective and timely disaster recovery and response planning. Decisions on resource deployment for search and rescue operations must be made with the best information available, often before visual damage assessments are available from the field. It is in this scenario, after evacuations have been completed but before recovery operations have begun, that the SLOSH model could benefit from initialization by surface stress fields forced by real-time surface wind analyses.

The purpose of this paper is to examine the observed and modeled wind and water-level response associated with the passage of TS Marco along Florida's west coast. Observed wind fields are representative of products that will be available in real time during and shortly after landfall. It is suggested that SLOSH model water-level response over short timescales can be improved by using real-time wind fields rather than the SLOSH model's current empirical wind profile.

2. Storm history

Tropical Storm Marco formed 55 km south-southwest of Key West, Florida, at 0600 UTC 10 October 1990 (Mayfield and Lawrence 1991). After forming, TS Marco moved northward during the next 2 days at approximately 4–5 m s^{-1} just west of the Florida peninsula (Fig. 1). The National Hurricane Center (NHC) estimated that Marco reached its peak intensity at 0800 UTC 11 October with a maximum sustained 1-min surface wind speed of 28 m s^{-1} and a minimum central pressure of 98.9 kPa. For the next several hours as Marco approached the coast, rapid fluctuations of water levels occurred along the Florida west coast and the Gulf of Mexico in response to wind forcing from Marco's rainbands. These bands also produced strong sustained winds and damaging gusts in areas near Sarasota Bay and Tampa Bay, Florida. After that time, nearly half of the storm's circulation was over land, and Marco weakened. The storm was downgraded to a tropical depression at 0000 UTC 12 October just before its center moved onshore near Cedar Key, Florida. Marco produced about $3 million of damage in Florida. Subsequently, the remnants of Marco and neighboring TS Klaus (Mayfield and Lawrence 1991) combined and produced an additional $54 million in damage from heavy rainfall and flooding, mainly over Georgia and the Carolinas.

3. Description of data and analysis

The number of low-level oceanic wind observations near the coast during Marco was relatively high in comparison with most hurricanes; strong winds did

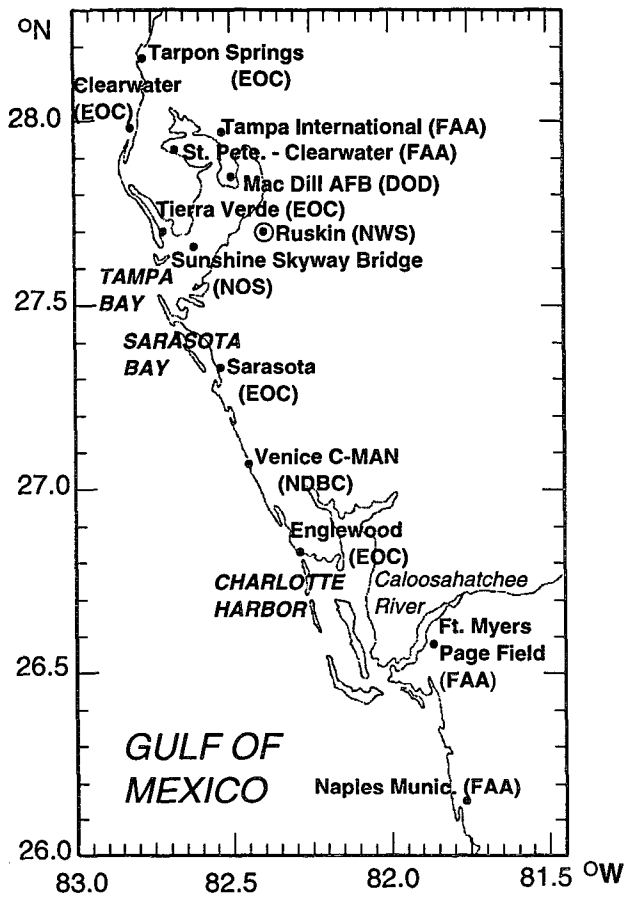

FIG. 2. Locations of stations reporting winds during TS Marco's passage. Ruskin, Florida, is the location of the NWS WSR-57 radar that recorded data used in this study.

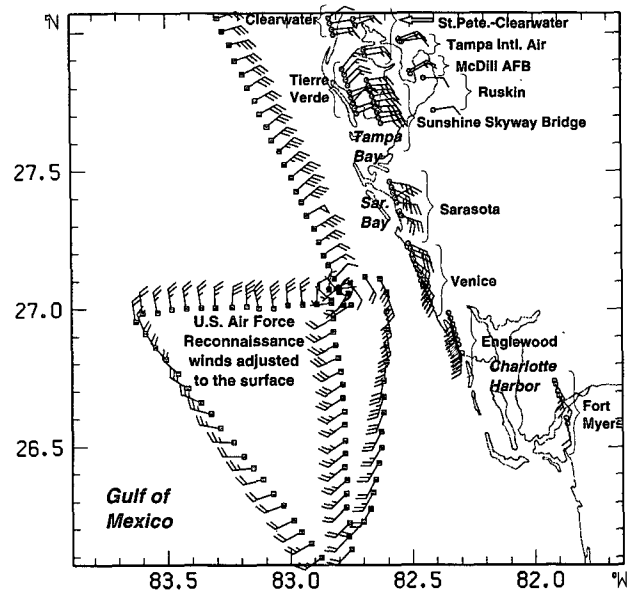

FIG. 3. Example of the surface wind observations and the air force reconnaissance flight-level winds adjusted to the surface. All observations are in storm-relative coordinates centered at 0800 UTC.

not destroy anemometers and the air force reconnaissance aircraft was able to collect low-level observations within the planetary boundary layer (PBL) at 0.5 km. Wind fields based on these observations were used to create time series of wind speeds and directions, which were compared with water-level measurements from a relatively dense network of coastal tide gauges.

a. Data sources and procedures

Surface wind observations were available from several sources (Fig. 2), including NWS, Department of Defense (DOD), Federal Aviation Administration (FAA), National Data Buoy Center (NDBC), NOS, and some Florida County Emergency Operations Center (EOC) offices. The averaging periods for the wind observations were 1 min for the NWS, DOD, and FAA stations and 10 min for the EOC, NOS, and NDBC's Venice C-MAN (Coastal-Marine Automated Network) platform sites.

Because the region affected by tropical storm winds is often too data sparse for an adequate analysis of the surface wind at a given time, all surface measurements were positioned in a storm-relative coordinate system over a period of 0.5–2 h. Aircraft-measured winds supplemented the surface data and were also positioned relative to the moving storm (Powell et al. 1991). An example of the data distribution in storm-relative coordinates is shown in Fig. 3. Aircraft wind data were obtained from U.S. Air Force reconnaissance aircraft via the Improved Weather Reconnaissance System (IWRS) that provides information on the location, strength, and intensity of tropical cyclones. The aircraft winds were 1-min means sampled every 10 s at altitudes of about 500 m over the Gulf of Mexico.

Radar reflectivity measurements of Marco's rainbands along the central Florida west coast were recorded by the WSR-57 radar at the Tampa Bay area NWS office in Ruskin, Florida (TBW), on the Radar Data Processor (RADAP II) as Video Integrator and Processor (VIP) levels (Saffle 1976). The VIP levels correspond to the ranges of reflectivity values shown in Table 1. Because there were some time periods with-

TABLE 1. The range of radar dBZ values and rainfall rate corresponding to the VIP levels used in the RADAP II system.

VIP levels	dBZ
1	18–29
2	30–40
3	41–45
4	46–49
5	50–56
6	57+

out RADAP II data, nearly continuous radar reflectivities recorded on 16-mm film were also obtained from the National Climatic Data Center (NCDC) for the TBW WSR-57 on 11 October.

Tide gauges in the area affected by Marco (Figs. 4a,b) were maintained by NOS, USGS, and some county EOC sites. Water-level fluctuations were recorded instantaneously every 6 min at the NOS gauges, 15 min at USGS gauges, and 10 min at EOC tide gauges.

b. Wind field analysis

1) ADJUSTMENT OF WIND DATA

Surface wind observations were adjusted to 10 m above the ground with an appropriate roughness length z_o using the log wind profile relationship for neutral conditions:

$$u_{10} = u_z \frac{\ln(10/z_o)}{\ln(z/z_o)}. \quad (1)$$

For anemometers on bridges or towers, z_o was set at 0.001 m for onshore flow, while in offshore flow, z_o was set at 0.03 m (airport exposure), based on roughness length descriptive categories (Panofsky and Dutton 1984).

Reconnaissance aircraft winds were adjusted from flight level to the surface with a PBL model described by Powell (1980). The PBL model estimates surface (10 m) wind speeds over water as a function of atmospheric stability conditions and surface stress. The inflow angle at the surface over the Gulf of Mexico was accounted for by backing the flight-level wind directions by 15°. This correction was based on averaging the difference in the wind direction between nearly collocated wind measurements at the surface (over water) and NOAA aircraft flying less than 1 km in tropical storms (about 15 years of these types comparisons were available).

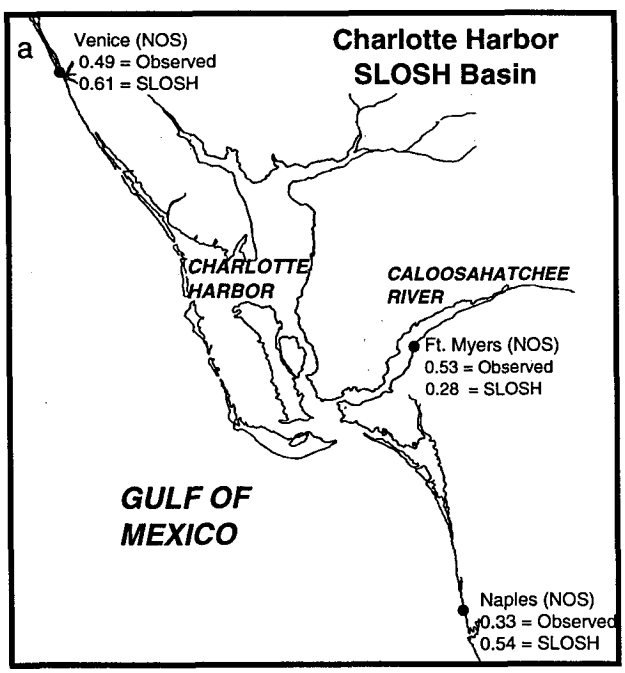

FIG. 4a. Portion of Charlotte Harbor SLOSH basin. Tide stations are shown with the maximum observed and the SLOSH model–calculated storm surge values (units = *m*) for TS Marco. The astronomical tides are *not* included in any of the storm surge values.

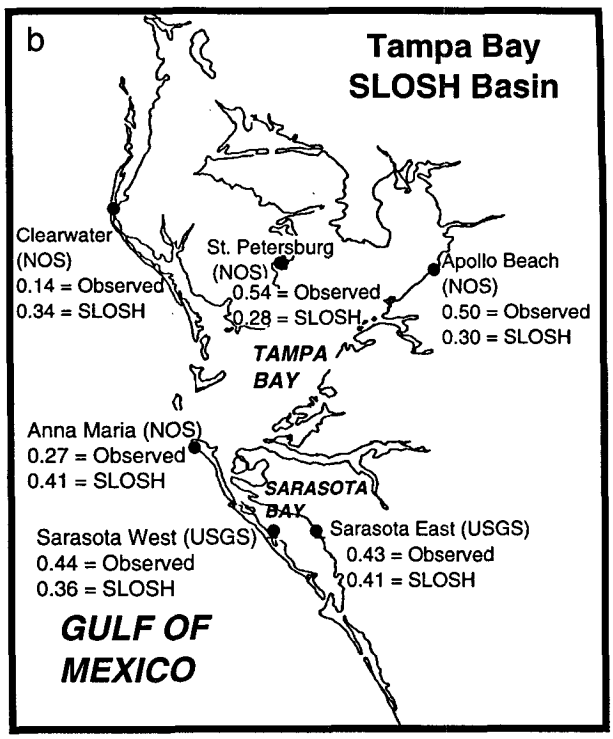

FIG. 4b. Same as Fig. 4a except this is a portion of the Tampa Bay SLOSH basin.

2) ANALYSIS METHOD FOR SURFACE WINDS

The analysis method for the surface and aircraft-adjusted winds was based on an objective scheme using the Spectral Application of Finite-Element Representation (SAFER) developed by Ooyama (1987) and described by Lord and Franklin (1987) and DeMaria et al. (1992). The SAFER method represents the dependent variables by a truncated series of cubic beta splines; the application of this technique to surface wind analyses was described by Powell et al. (1991). The input wind data spacing and averaging times represent both resolvable and undersampled scales of motion. The surface wind analysis produces a low-pass-filtered mesoscale wind field with high frequency and with small-scale wind features removed.

This technique is currently being developed by the Hurricane Research Division (HRD) as a surface wind analysis system for evaluation and eventual transfer to NHC. For storm surge and wave modeling, the 10-min mean wind is considered to be more representative of timescales associated with ocean response to surface stress. Also, the SLOSH model wind speeds are considered to be roughly equivalent to 10-min average winds (C. Jelesnianski 1993, personal communication). Therefore, for comparison purposes, the mesoscale analysis wind fields were adjusted to produce maximum 10-min average winds, V_{M10}. This was accomplished by developing a 10-min gust factor relationship (G_{10}) based on the of the approach of Durst (1960) and Krayer and Marshall (1992) using data gathered from all C-MAN stations with continuous 10-min wind measurement capability in all tropical cyclones since 1985. This gust factor relationship was applied to restore the amplitude of the mesoscale wind field to an estimate of the maximum 10-min wind that would have occurred over a time period t given by the ratio of twice the analysis filter wavelength λ to the low-pass-filtered analysis wind speed, V_{MESO} [i.e., $t = (2\lambda)/V_{MESO}$]. The expression for the gust factor is

$$G_{10} = 1.0 + 0.333 \times 10^{-4}\,(t - 600), \qquad (2)$$

where t is in seconds and it is assumed that if $t \leq 600$ s, then $G_{10} = 1.0$, or if $t > 3600$ s, then $G_{10} = 1.1$.

For Marco, each analysis consisted of 21×21 grid points in the 222-km $\times$ 222-km domain centered on the storm as it tracked northward. After the initial surface wind analysis for 0100 UTC 11 October was computed, each subsequent analysis included the background field sampled from the previous wind analysis as input (e.g., the 0100 UTC background field was used in the 0145 UTC analysis). Small periods of 0.5–2.0 h were chosen for the input data time window of individual analyses. Short time intervals between analyses were chosen to minimize the likelihood that observations from sites with over-water exposure would be relocated onshore when transformed into storm-relative coordinates. For example, the over-water observations from Sunshine Skyway Bridge (Fig. 2) over the southern portion of Tampa Bay would have translated northward greater than 32 km for time periods longer than 2 h, which would have carried them inland to the St. Petersburg area. Similarly, some over-land exposures (e.g., Sarasota) would be carried offshore for longer time intervals when transformed into storm-relative coordinates. The value of λ used was 39 km, which was chosen to allow the resolution of mesoscale features, such as the vortex and rainband wind maxima (described by Powell 1990). The chosen value of λ also reduced observational noise associated with exposure and sampling differences, including small-scale wind features (e.g., turbulent and convective gusts and lulls) that cannot be adequately resolved by the available observations. Based on the value of λ (39 km) and typical amplitudes of V_{MESO} (15–25 m s^{-1}), the timescales for the mesoscale winds range from 52 to 87 min [e.g., $t = (2 \cdot 39 \times 10^3\ \text{m})/23\ \text{m s}^{-1} = 3391$ s or 56.5 min]. Hence, the value of G_{10} applicable for $V_{MESO} = 23.0$ m s^{-1} would be 1.09, resulting in $V_{M10} = 25.1$ m s^{-1}.

c. *SLOSH model wind and surge prediction*

HRD wind analyses were compared with those predicted by the SLOSH model at tide gauges located in the two SLOSH basins affected by Marco: Charlotte Harbor, Florida (Fig. 4a), and Tampa Bay (Fig. 4b). The wind model used in SLOSH evolved from that used in the Special Program to List Amplitudes of Surges from Hurricanes (SPLASH) according to Jelesnianski and Taylor (1973) and Jelesnianski et al. (1992). The pressure and wind direction are computed for a stationary, circularly symmetric storm using the balance of forces along a surface wind trajectory [(3)] and normal to a surface wind trajectory [(4)] adapted from Myers and Malkin (1961):

$$\underbrace{\frac{1}{\rho_s}\frac{dp}{dr}}_{\text{(pres. grad.)}} = \underbrace{\frac{k_s V^2}{\sin\Phi}}_{\text{(friction)}} - \underbrace{V\frac{dV}{dr}}_{\text{(centrifugal)}} \qquad \text{[along trajectory]} \quad (3)$$

$$\underbrace{\frac{1}{\rho_a}\frac{dp}{dr}}_{\text{(pres. grad.)}}\cos\phi = \underbrace{fV}_{\text{(Coriolis)}} \underbrace{\frac{V^2}{r}\cos\Phi - V^2\frac{d\Phi}{dr}\sin\Phi}_{\text{(2 centrifugal terms)}} + \underbrace{k_n V^2}_{\text{(friction)}}$$

$$\text{[normal to trajectory]}, \quad (4)$$

where r is the distance from the storm center, $p(r)$ is the pressure (p_a is the central pressure), $\Phi(r)$ is the inflow angle across circular isobars toward the storm center, $V(r)$ is the wind speed profile, and f is the Coriolis parameter. The streamwise and normal components of the vertical stress gradient are parameterized with friction coefficients, k_s and k_n, which are directly proportional to the R_{MW} and inversely proportional to the maximum wind speed (V_{RMW}). According to Jelesnianski et al. (1992), these coefficients were not designed specifically to produce accurate wind fields but to produce well-behaved winds to make surge forecasts. The friction coefficients are independent of the drag coefficient used to compute surface stress, which is assumed constant at 3.0×10^{-3}. The SLOSH model uses the following wind speed profile for a stationary storm:

$$V(r) = V_{RMW}\frac{2(R_{MW})r}{(R_{MW})^2 + r^2}. \qquad (5)$$

TABLE 2. Input parameters for the SLOSH model wind field. The storm's track is input for 6-h intervals along with the pressure deficit (Δp) and R_{MW}.

Date	Time (UTC)	Lat (°N)	Long (°W)	Δp (kPa)	RMW (km)
10 Oct	1800	25.2	82.5	1.6	26.0
11 Oct	0000	26.0	82.6	1.7	29.0
11 Oct	0600	26.7	82.6	2.1	26.0
11 Oct	1200	27.5	82.8	1.6	31.0
11 Oct	1800	28.3	83.0	1.2	35.0
12 Oct	0000	29.1	83.1	1.1	40.0

Jelesnianski et al. (1992) claim that in reality forecasts of V_{RMW} are often not readily available over the ocean and forecasts of vector wind fields are not available for all storms in all areas. The basic design philosophy of SLOSH is to avoid uncertainties associated with input fields derived from hurricane wind and pressure measurements and to allow surge computations to be made with limited knowledge of the storm's structure and intensity. This is accomplished by concentrating on deriving a surface pressure and wind direction field consistent with a hypothetical radial wind speed profile (5) based on the observed radius of maximum winds and the large-scale pressure gradient. An iterative procedure solves (3) and (4) if estimates are available for the central and environmental pressure and R_{MW}; V_{RMW} is first approximated using empirically derived tables, and the balance equations are then solved for $p(r)$ and $\Phi(r)$. For each iteration, V_{RMW} is changed until the pressure discrepancy is less than an arbitrary threshold value. The model uses two different coefficients of friction: one for over ocean and the other for offshore flow or inland over-water conditions, such as flow across bays or lakes (these are referred to as "lake winds"). Given the wind directions from (3) and (4), and the surface wind speed (including a simple correction for the forward motion of the storm) from (5), the surface stress field is computed using the drag coefficient. The surge height at a given grid point is then computed by integrating the water transport equations (with water movement forced by the surface stress, bottom stress, and the horizontal surface pressure gradient) and finally the continuity equation for the height of the water surface (forced by net convergence of water into a grid volume).

For this study, the SLOSH model runs were initialized with TS Marco's "best-track" positions (Mayfield and Lawrence 1991) and estimates of the pressure deficit (e.g., the pressure deficit Δp is 2.1 kPa if the environmental pressure is 101.0 kPa and the storm's central pressure is 98.9 kPa). The R_{MW} was based on the HRD analysis wind fields at intervals of 6 h (Table 2). The SLOSH model runs computed the maximum storm surge for each grid point, as well as time series of the model's storm surge (astronomical tides were not included) and wind speed and direction. These are normally output only at predefined locations related to emergency management evacuation concerns. These gridpoint values are normally output at 30-min intervals (note this is *not* the model's "time step").

The wind profile for a slice extending to the right from the center for 1200 UTC 11 October is shown in Fig. 5 for the HRD V_{M10} winds and the SLOSH model winds. The profile contains the maximum wind (R_{MW} = 31 km at 1200 UTC according to Table 2) and, because Marco was moving almost due north at this time, the highest winds are approximately due east of the center. The analyzed and model wind profiles to the east of the storm center are in very good agreement for the portion of the radial distance from the storm's center to the R_{MW}. However, for radial distances beyond the R_{MW}, the HRD analysis wind profile, which is over land east of Tampa Bay, decreases much more rapidly than the SLOSH-calculated winds, which are always considered to have an over-inland-water (i.e., lake winds) fetch.

A total of 17 HRD V_{M10} analyses were made from the input data over the time period from 0100 to 1545 UTC 11 October. The HRD V_{M10} analyses were sufficient to construct onshore and offshore wind velocity component time series at about 1-h resolution for comparison to SLOSH model gridpoint values (time series of the alongshore wind velocity components, which were also constructed, are not shown). Comparisons of the SLOSH-predicted time series of storm surge with the observed storm surge together with comparisons of the SLOSH and HRD analysis wind time series determined whether inaccurate SLOSH

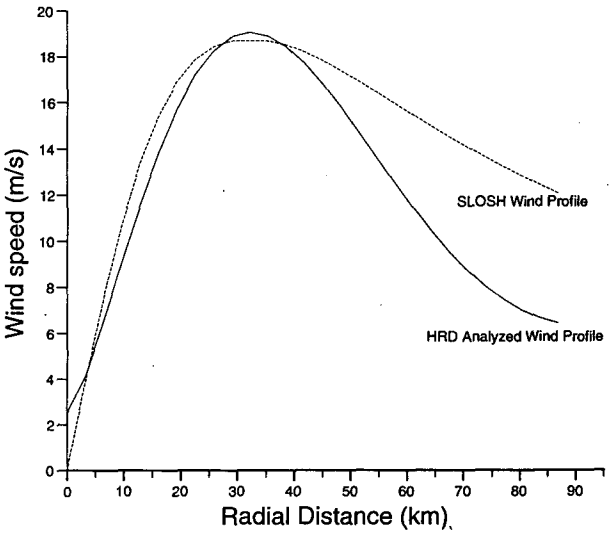

FIG. 5. HRD V_{M10} (solid) and SLOSH model (dashed) radial wind lake wind profile (forward motion of the storm is included) for TS Marco at 1200 UTC 11 October. The wind profile extends eastward from the storm center (located at 0 km); within 31 km of the center, the profile is over Tampa Bay, but the remainder of the profile is over land greater than 31 km.

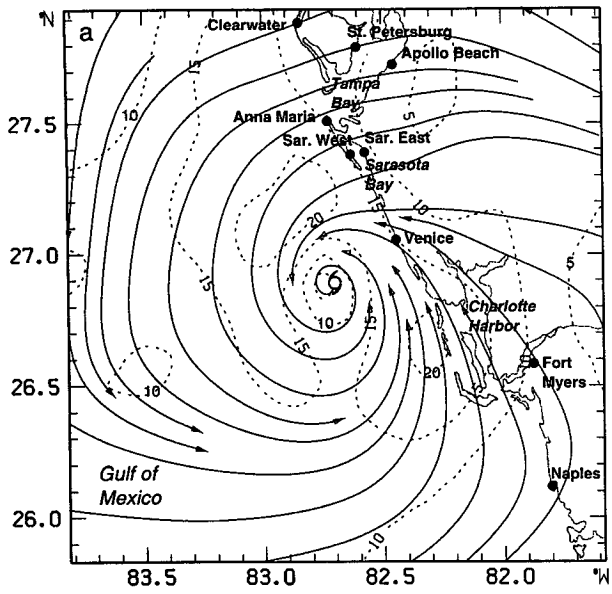

FIG. 6a. HRD-analyzed V_{M10} field for TS Marco at 0630 UTC 11 October 1990; streamlines and isotachs (contour interval = 5 m s^{-1}) are shown. The wind field is earth relative.

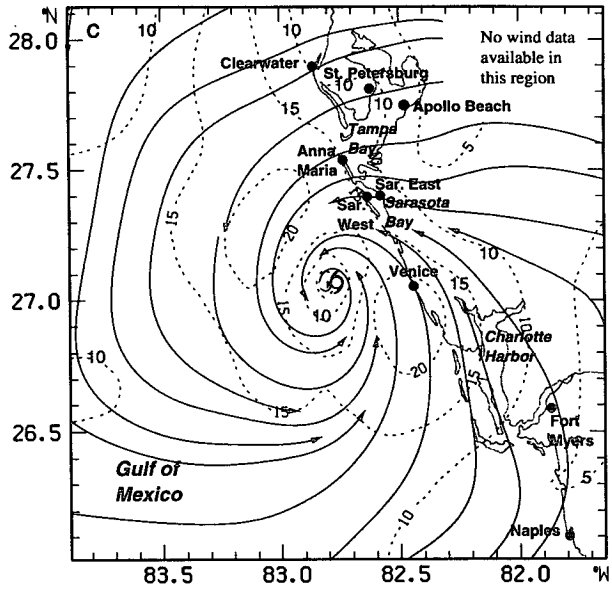

FIG. 6c. Same as Fig. 6a except at 0800 UTC.

wind forcing may have been associated with deviations of the predicted surge from the observed surge.

4. Atmospheric forcing and storm surge

a. Venice and Sarasota Bay

Marco's circulation covered the west-central coastline of Florida, including Sarasota Bay and most of Tampa Bay at 0630 UTC (Fig. 6a). The HRD V_{M10} wind field indicated greater than 20 m s^{-1} northwest of the center, while along the coast a region of V_{M10} > 20 m s^{-1} was at the entrance to and west of Charlotte Harbor. Winds in excess of gale force (>18 m s^{-1}) were just offshore from near Venice through Sarasota Bay. Radar reflectivities recorded at TBW (Fig. 6b) showed a broad area of rain in an area oriented northwest–southeast from Sarasota Bay to Charlotte Harbor at 0630 UTC.

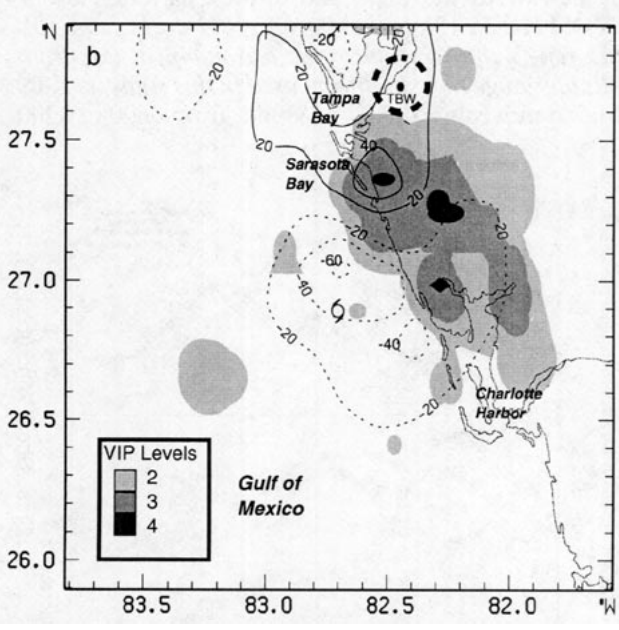

FIG. 6b. Radar reflectivities from the NWS radar at Ruskin at 0630 UTC. These radar echoes were recorded as VIP levels defined in Table 1. The contours show areas of divergence (contour interval = 20 × 10^{-5} s^{-1}) based on analyzed V_{MESO} fields; dashed contours indicate negative values or convergence.

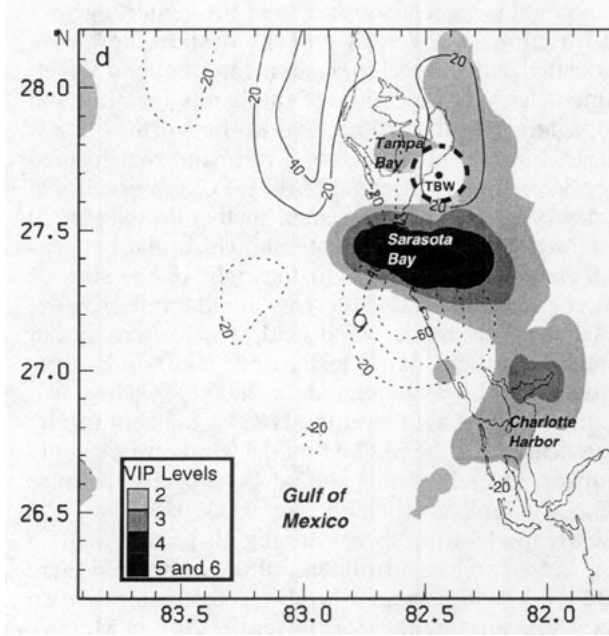

FIG. 6d. Same as Fig. 6b except at 0900 UTC.

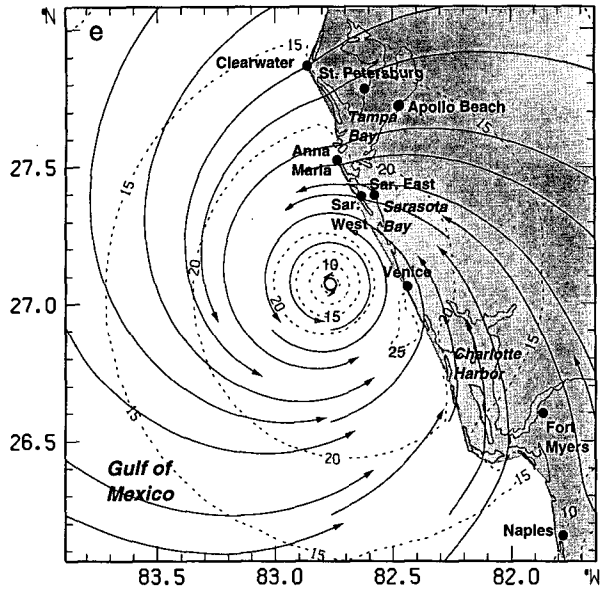

FIG. 6e. SLOSH model wind field for 0800 UTC. (Ocean winds are over the Gulf of Mexico and the shaded areas indicate lake winds over land areas and bays.)

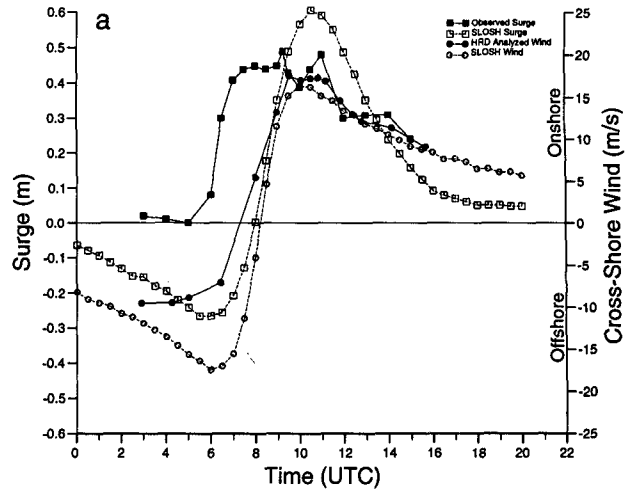

FIG. 7a. Time series (UTC) on 11 October of storm surge (m) and cross-shore winds (m s^{-1}) based on the HRD V_{M10} fields (*onshore flow* > 0, *offshore flow* < 0). This tide gauge is operated by NOS at Venice. The solid curves are the HRD-analyzed cross-shore wind speeds and the observed storm surge, while the dashed curves indicate the SLOSH model output.

The magnitude and areal coverage of the radar reflectivities expanded rapidly in a rainband along the coast in the right front quadrant of the storm (i.e., northeast of the storm's center) near Venice during 0700–0800 UTC. The rainband propagated northward where it continued to increase in both area and intensity. During this period (Fig. 6c), Marco intensified, reaching its lowest central pressure of 98.9 kPa and peak maximum sustained wind speed of about 28 m s^{-1} (Mayfield and Lawrence 1991). Strong southerly winds to the right (i.e., east-southeast) of the center together with frictional convergence of the onshore flow were associated with a preferred area for rainband development with a succession of rainbands forming and propagating northward relative to the storm. For example, Fig. 6d shows a second rainband that formed over Sarasota Bay at about 0900 UTC. Observational studies of landfalling hurricanes, such as Powell (1982) and Parrish et al. (1982), have shown similar patterns of increased convergence to the right of the storm's center and an associated increase in radar reflectivities.

The SLOSH model wind field, which used "ocean winds" over the Gulf of Mexico and "lake winds" over land and bays, was generated for 0800 UTC (Fig. 6e). Comparing this field with the HRD V_{M10} field in Fig. 6c indicates that the SLOSH model winds are generally stronger. Over land this should be expected because "lake friction" coefficients are used. However, the SLOSH model wind speeds are slightly greater than 25 m s^{-1} in an area east-southeast of the center and there is 32–50-km-wide band of wind speeds greater than 20 m s^{-1} surrounding the storm over the Gulf of Mexico. This band is not present in the HRD V_{M10} field, so the SLOSH winds appear to be overestimating the winds west and southwest of the storm center by about 5 m s^{-1}.

Time series of the observed and SLOSH model–calculated storm surge and the HRD V_{M10} and SLOSH model winds for Venice are presented in Fig. 7a. The tide gauge at Venice (Fig. 4a) is located along the coast at the extreme northern part of the Charlotte Harbor SLOSH basin. (*Note that the observed storm surge values reflect the removal of the astronomical tide from* ***all*** *tide gauge measurements used in this study.*) As TS Marco moved northwest of Venice from 0600 to 0900

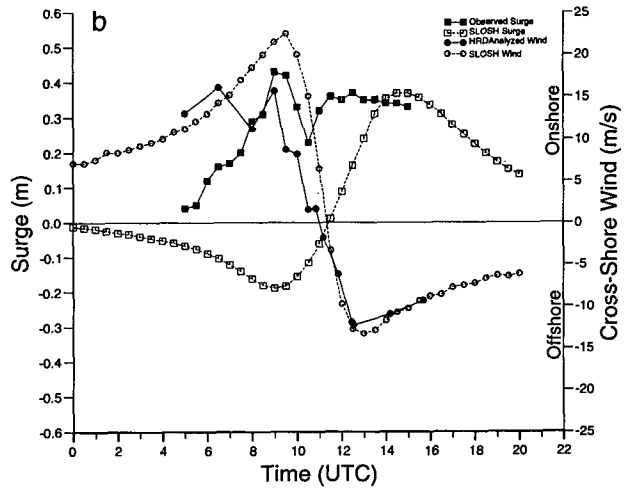

FIG. 7b. Same as Fig. 7a except for USGS tide gauge at Sarasota Bay west.

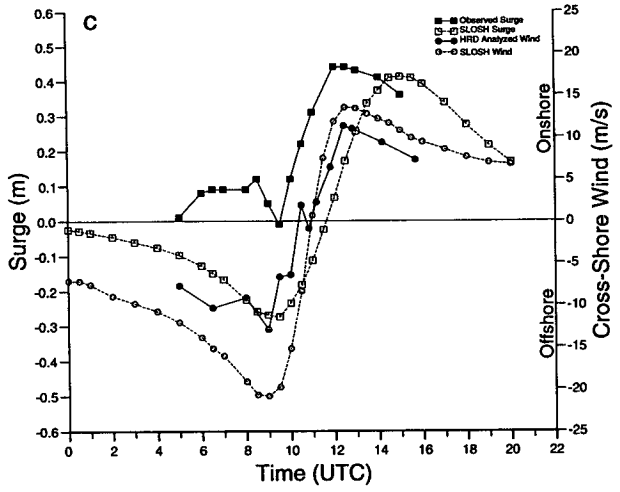

FIG. 7c. Same as Fig. 7a except for USGS tide gauge at Sarasota Bay east.

UTC, the cross-shore component of the wind changed rapidly from offshore to onshore, while the onshore component of the SLOSH model winds did not begin until after 0800 UTC. The SLOSH-calculated wind at Venice represented "over-lake" flow before 0800 UTC, when the cross-shore wind component was offshore. This resulted in SLOSH computing a negative storm surge, but in reality the observed surge was never negative, because the observed offshore winds were reduced due to the friction effects from the land surface. After 0800 UTC, observed and SLOSH-calculated cross-shore wind components were in very close agreement with peaks of about 20 m s^{-1} in onshore flow. The maximum observed and model-calculated storm surges occurred at about 1000 UTC, although the model indicated the peak surge should be 20% higher.

Farther up the coast from Venice is Sarasota Bay, which is a relatively small bay with restricted flow through a series of inlets to the Gulf of Mexico. In the western part of the bay, easterly winds (onshore flow at this location) ahead of the rainband pushed water across the bay onto the barrier island (Fig. 7b). At this time the SLOSH model indicated negative storm surge values, but wave effects may have contributed to some of the observed storm surge. On the east side of Sarasota Bay (Fig. 7c) water levels dropped due to the strong easterly winds (offshore flow at this location) at about 0900 UTC. However, as Marco continued northward, the maximum winds behind the rainband became southerly, and water flowed rapidly into Sarasota Bay from the Gulf of Mexico. This onshore wind flow caused the water levels on the east side of the bay to peak at about 1200 UTC. The SLOSH-calculated peak storm surge was approximately the same magnitude as that observed but was lagged about 3 h. The time series of the offshore–onshore components of the wind at Sarasota east compare to within ±2 m s^{-1} after 1000 UTC but differ by several meters per second before this time due to the offshore component of the HRD V_{M10} winds being more representative of over-land upwind fetch. These strong offshore SLOSH model winds preceding the storm probably caused the model to force too much water out of Sarasota Bay into the Gulf of Mexico, which resulted in a longer period of time required to force the water back into the bay to achieve a realistic maximum storm surge.

b. *Tampa Bay*

The HRD V_{M10} field indicated a decrease in wind speeds by 1200 UTC (Fig. 8a) as Marco's circulation extended farther inland. However, a very strong rainband (Fig. 8b) over Tampa Bay produced wind gusts to 31 m s^{-1} at MacDill Air Force Base at 1220 UTC as it moved northward. Later wind analyses (not shown) indicate that southwesterly winds occurred at the mouth of Tampa Bay from 1300 to 1530 UTC.

The SLOSH model wind field for 1200 UTC (Fig. 8c) also showed a decrease in the wind speed around the storm (note that the profiles shown in Fig. 5 are for this time). Both the SLOSH and HRD V_{M10} (Fig. 8a) fields show wind speeds about 15 m s^{-1} over the lower portion of Tampa Bay. The SLOSH model "ocean winds" over the Gulf of Mexico are again larger than the HRD V_{M10} winds, which are greater than 15 m s^{-1} northwest and southeast of the center.

At the Apollo Beach tide gauge in Tampa Bay (Fig. 9a) the surge fell to a negative minimum at about 1230 UTC as the rainband in Fig. 8b moved across Tampa Bay. The cross-shore component for both the HRD analysis and SLOSH-modeled winds were directed off-

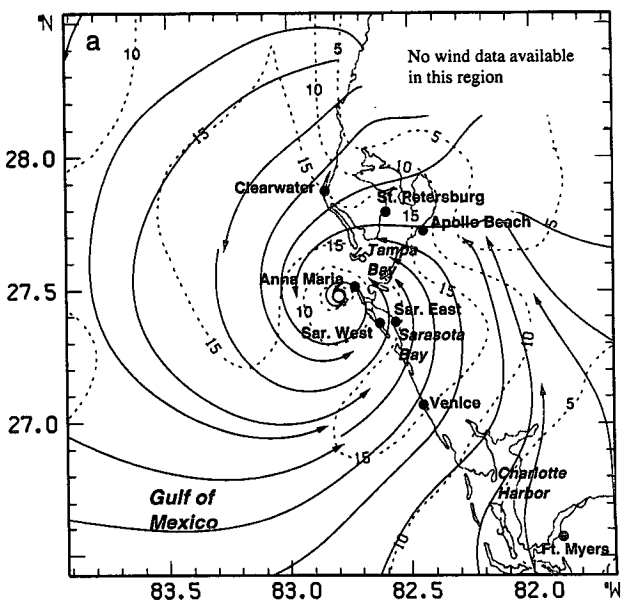

FIG. 8a. Same as Fig. 6a except at 1200 UTC.

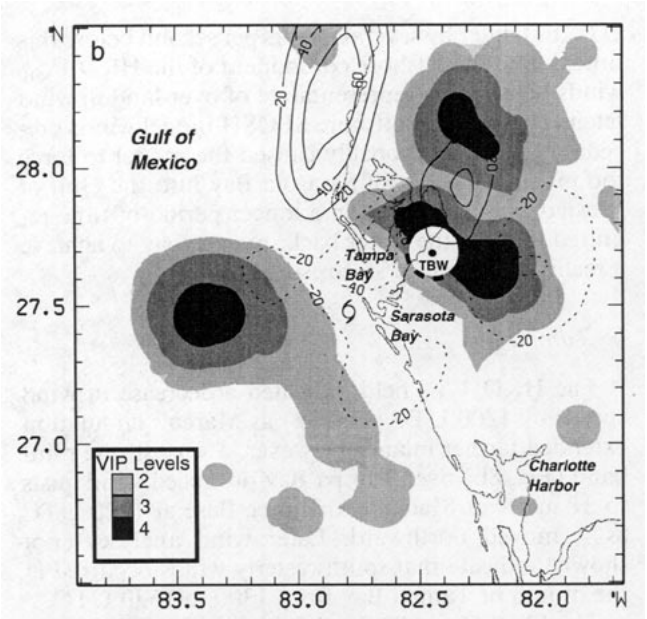

FIG. 8b. Same as Fig. 6b except at 1200 UTC.

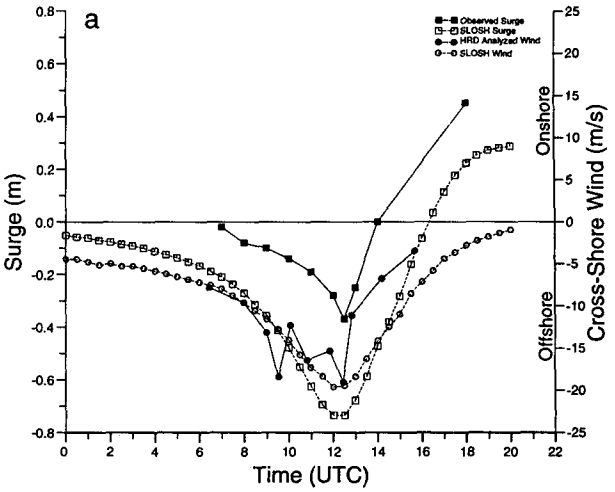

FIG. 9a. Same as Fig. 7a except for NOS tide gauge at Apollo Beach.

shore during this time. The peak observed and modeled surge occurred several hours later at about 1800 UTC. Directly across Tampa Bay at the St. Petersburg NOS tide gauge the surge reached its peak about the same time the large negative surge occurred at Apollo Beach (Fig. 9b). At this time the onshore wind component at St. Petersburg increased to about 18 m s^{-1}. The rapid increase in observed storm surge over northern Tampa Bay during 1100–1230 UTC was probably due to strong winds associated with the rainband (Fig. 8b), which moved northward across the area at approximately that time (waves may have contributed to some of the observed storm surge). The SLOSH-computed surge was negative at the time of the observed peak surge and did not produce positive values until after 1600 UTC. Despite stronger offshore SLOSH winds at Apollo Beach, and close to observed SLOSH winds at St. Petersburg, predicted surge heights at St. Petersburg were out of phase with nearly 1-m difference in magnitude. This is likely related to a water flow problem in modeling Tampa Bay rather than a wind forcing problem.

5. Discussion and conclusions

The comparisons of the analyzed and modeled winds and storm surge for TS Marco show that in general the

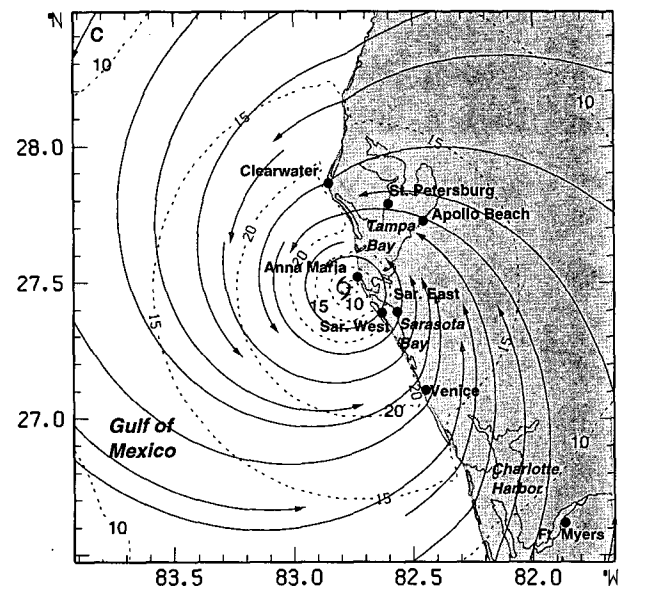

FIG. 8c. Same as Fig. 6e except at 1200 UTC.

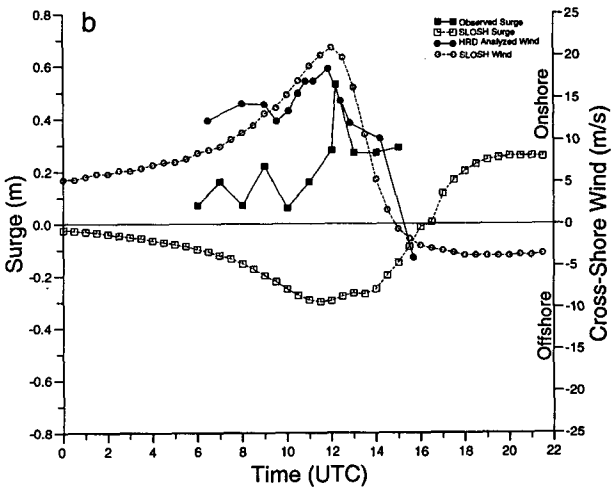

FIG. 9b. Same as Fig. 7a except for NOS tide gauge at St. Petersburg.

SLOSH model reasonably represented the maximum storm surge for a tropical storm in two basins with relatively complicated coastlines. The differences between the maximum observed and SLOSH model storm surge ranged from an overestimate of 0.21 m at Naples to an underestimate of 0.26 m at St. Petersburg. Time series of the model and observed storm surges indicated that the model performed best at Venice where the tide gauge was on the open Gulf of Mexico, with no restrictions to flow like those observed in Sarasota Bay and Tampa Bay. However, even at Venice the SLOSH model storm surge was 20% higher than the observed storm surge. The model performed poorly in areas of offshore flow because it overestimated the surface winds resulting in predictions of excessive negative surge (e.g., at St. Petersburg there was about a 0.9-m difference between the actual and SLOSH model surge at the time of the observed maximum surge). This may be important in small bays during episodes of winds that shift from offshore to onshore as a storm passes. Loss of too much water due to overpredicted offshore winds may result in time lags of maximum surge height once the wind shifts back to onshore.

Marco intensified and formed strong rainbands in the front right quadrant of the storm when the onshore flow portion of its circulation reached the coastline. This is a characteristic feature of landfalling storms and has been attributed to frictional convergence. The wind maximum to the right of the center was located just below the rainband area but was in the same general area that highest winds would be expected on the basis of circulation and translation alone. Hence SLOSH winds resolved the maximum well, provided the wind direction was not offshore. In cases where convective rainbands produce wind asymmetries in locations relative to the storm that are not well modeled by translation and circulation, short-period water-level fluctuations would not be expected to be resolved in the SLOSH wind profile; there is no provision for cloud parameterization and convective motion feedback. This is an important consideration in hurricanes where secondary wind maxima associated with concentric and spiral rainbands are dominant features in the wind field (e.g., Willoughby et al. 1982). If model limitations are noticeable in relatively weak tropical storms, problems with even larger magnitudes may be possible in intense hurricanes. Similar case studies of hurricanes with asymmetric wind fields are needed to further document problems with rainbands and the lag in surge response to the winds changing from offshore to onshore.

Although the SLOSH model can be run in advance of a tropical cyclone affecting a particular coastline, for emergency evacuation purposes, the results must be received 24–36 h before landfall. For such lead times, it is not possible to accurately forecast the time evolution of the water levels; the maximum surge is the most important quantity that determines evacuation zones. During the time preceding landfall, rapid changes in the intensity and/or track of the storm often occur. These changes could bring storm surges of different magnitudes and at different locations than those predicted 12–24 h earlier. Because of the current uncertainty in tropical cyclone track and intensity forecasts, real-time SLOSH forecasts are not practical until the 0–6-h period.

Most landfalling storms affecting North America and much of the Caribbean are monitored by reconnaissance aircraft flown by the U.S. Air Force or NOAA. These aircraft now have sophisticated inertial navigation systems and satellite links for delivering data to NHC for input to real-time analysis. New remote sensing platforms being developed and tested on NOAA aircraft include surface wind sensing radiometers and scatterometers and real-time processed winds at 500 m above the surface from airborne Doppler radars. Satellite radiometers and scatterometers are continuing to evolve and may eventually be capable of supplementing hurricane wind field measurements. For real-time use, this study has shown that the incorporation of analyzed wind fields based on these data would provide a potential area for improvement in the SLOSH model. Such fields were not readily available when the SLOSH model was conceived but they soon will be available in real time. At the very least, these analyses can be used to estimate the R_{MW} 0–12 h in advance of landfall. The R_{MW} and the pressure deficit are critical parameters in the SLOSH model wind field. Alternatively, real-time analyzed wind fields transformed to the model grid domain would more realistically fit observed wind field asymmetries associated with rainband convection, storm motion, and the surrounding environmental flow that are not resolvable by the SLOSH wind profile. Successful use of these fields would require changes in the underlying philosophy and initialization of the SLOSH model, so that the model would be based on the observed wind field. Potential changes to investigate might also include 1) given surface wind fields every 6 h and sufficient boundary conditions, the computation and use of the divergence, vorticity, and time and space derivatives of the divergence field to solve the divergence equation for the pressure field, and 2) the incorporation of recent developments in the surface drag coefficient parameterization as a function of wind velocity and wave age (e.g., Janssen 1991). This step might incorporate a state-of-the-art wave model to allow feedback from a changing wave field on the surface stress such as the third-generation wave prediction model (WAM) developed by the WAMDI Group (1988).

As the point of landfall becomes more certain, some further refinement of the storm surge predictions, based on real-time analyzed surface wind fields, could be provided to the emergency officials during their final preparations and could allow them to concentrate on response and recovery planning and potential locations for search and rescue efforts. Real-time surface wind

analyses are also critical for preliminary damage assessment purposes immediately following landfall. SLOSH model predictions using input parameters based on real-time wind analyses could be used to determine the areas inundated by storm surge with the results available immediately following the storm. With the availability of preliminary maximum wind swath and storm surge inundation maps, federal, state, and local government recovery efforts could be focused on areas requiring immediate attention.

Acknowledgments. This work was partially funded by NOAA's Coastal Ocean Program. Some of the data used in this study were provided by NWS offices at Ruskin and Miami, Florida. R. Balfour, MIC at Ruskin, was especially helpful with leads for locating data sources. C. Paxton, also at Ruskin, provided the RADAP II data; microfilm from the Ruskin WSR-57 radar were obtained from NCDC. R. Merrill of the University of Wisconsin provided satellite data. R. Leep of WTVT provided recorded data from the station's Doppler radar. M. Rutstein of NOS provided tide data, and E. Meindl of NDBC provided the Venice C-MAN data. The USGS tide data were provided by D. Schoellhamer and P. Boetcher. The EOC wind and tide data were provided by G. Vickers of Pinellas County and L. Stevens of Sarasota County. J. Hudson of The Florida State University provided data for the first-order stations, and Sgt. Holtgard provided the MacDill Air Force Base wind observations. Special thanks go to W. Shaffer of NOAA's Techniques Development Laboratory, who provided the code for the SLOSH model wind field, M. Mayfield who prepared NHC's Preliminary Report on this storm, and S. Peene at the University of Florida for his help with interpreting much of the tide data used. The following individuals at the Hurricane Research Division provided assistance with this study: V. Wiggert for running the SLOSH model, S. Aberson and S. Feuer for help with wind analyses, P. Dodge for help with analyzing radar data, L. Shapiro for error analysis and interpretation of the SLOSH wind model, J. Berkeley for archiving much of the wind and tide data, and J. Griffin and M. Black for decoding and displaying the satellite data. Reviews of this manuscript by V. Wiggert, P. Dodge, R. Burpee, W. Shaffer, G. Barnes, and an anonymous reviewer were very helpful.

APPENDIX

Summary of Abbreviations

Φ	inflow angle across isobars toward the storm center
λ	filter wavelength
f	Coriolis parameter
G_{10}	gust factor used to convert analyzed mesoscale wind to 10-min wind
k_s and k_n	friction coefficients along and normal to streamlines, respectively
$p(r)$	pressure (p_a is the central pressure)
r	distance from the storm center
R_{MW}	radius of maximum wind
t	timescale used to determine maximum sustained 10-min wind
u_z	wind speed at height z above surface (u_{10} for z = 10 m)
$V(r)$	surface wind speed profile
V_{M10}	maximum sustained surface wind speed for 10 min
V_{MESO}	mesoscale surface wind speed
V_{RMW}	surface wind speed at the R_{MW}
z	height above surface
z_o	roughness length
C-MAN	Coastal-Marine Automated Network
DOD	Department of Defense
EOC	Emergency Operation Center
FAA	Federal Aviation Administration
HRD	Hurricane Research Division
IWRS	Improved Weather Reconnaissance System
MEOW	Maximum Envelope of Water
NCDC	National Climatic Data Center
NDBC	National Data Buoy Center
NHC	National Hurricane Center
NOS	National Ocean Service
NWS	National Weather Service
PBL	planetary boundary layer
RADAP II	Radar Data Processor
SAFER	Spectral Application of Finite-Element Representation
SLOSH	Sea, Lake, and Overland Surge from Hurricanes
TBW	Ruskin, Florida (NWS)
TS	tropical storm
USGS	United States Geological Survey
UTC	universal time coordinated
VIP	Video Integrator and Processor

REFERENCES

DeMaria, M., S. M. Aberson, K. V. Ooyama, and S. J. Lord, 1992: A nested spectral model for hurricane track forecasting. *Mon. Wea. Rev.*, **120,** 1628–1643.

Durst, C. S., 1960: Wind speeds over short periods of time. *Meteor. Mag.*, **89,** 181–186.

Janssen, P. A. E. M., 1991: Quasi-linear theory of wind-wave generation applied to wave forecasting. *J. Phys. Oceanogr.*, **21,** 1631–1642.

Jarrell, J. D., P. J. Hebert, and M. Mayfield, 1992: Hurricane experience levels of coastal county populations, Texas to Maine. NOAA Tech. Memo./NWS-NHC 46, Coral Gables, FL, 152 pp.

Jarvinen, B. R., and M. B. Lawrence, 1985: An evaluation of the SLOSH storm surge model. *Bull. Amer. Meteor. Soc.*, **66,** 1408–1411.

——, and J. Gebert, 1986: Comparison of observed versus SLOSH model computed storm surge hydrographs along the Delaware and New Jersey shorelines for Hurricane Gloria, September 1985. NOAA Tech. Memo. NWS NHC 32, Coral Gables, FL, 17 pp.

——, and ——, 1987: Observed versus SLOSH model storm surge for Connecticut, New York, and upper New Jersey in Hurricane

Gloria, September 1985. NOAA Tech. Memo. NWS NHC 36, Coral Gables, FL, 17 pp.

——, and A. McDuffie, 1987: Observed versus SLOSH model storm surge for North Carolina in Hurricane Gloria, September 1985. NOAA Tech. Memo. NWS NHC 37, Coral Gables, FL, 21 pp.

Jelesnianski, C. P., and A. D. Taylor, 1973: A preliminary view of storm surges before and after storm modifications. NOAA Tech. Memo. ERL WMPO-3, Boulder, CO, 33 pp.

——, J. Chen, and W. A. Shaffer, 1992: SLOSH: Sea, Lake, and Overland Surges from Hurricanes. NOAA Tech. Rep. NWS 48, Silver Spring, MD, 71 pp.

Krayer, W. R., and R. D. Marshall, 1992: Gust factors applied to hurricane winds. *Bull. Amer. Meteor. Soc.*, **73,** 613–617.

Lord, S. J., and J. L. Franklin, 1987: The environment of Hurricane Debbie. Part I: Winds. *Mon. Wea. Rev.*, **115,** 2760–2780.

Mayfield, M., and M. B. Lawrence, 1991: Atlantic hurricane season of 1990. *Mon. Wea. Rev.*, **119,** 2760–2780.

McAdie, C. J., and M. B. Lawrence, 1993: Long-term trends in National Hurricane Center track forecast errors in the Atlantic basin. Preprints, *20th Conf. on Hurricanes and Tropical Meteorology,* San Antonio, TX, Amer. Meteor. Soc., 281–284.

Myers, V. A., and W. Malkin, 1961: Some properties of hurricane wind fields as deduced from trajectories. National Hurricane Research Project Report, No. 49, NOAA, U.S. Department of Commerce, 43 pp.

Ooyama, K. V., 1987: Scale-controlled objective analysis. *Mon. Wea. Rev.*, **115,** 2479–2506.

Panofsky, H. A., and J. A. Dutton, 1984: *Atmospheric Turbulence: Models and Methods for Engineering Applications.* Wiley, 397 pp.

Parrish, J. R., R. W. Burpee, F. D. Marks Jr., and R. Grebe, 1982: Rainfall patterns observed by digitized radar during landfall of Hurricane Frederic (1979). *Mon. Wea. Rev.*, **110,** 1933–1944.

Powell, M. D., 1980: Evaluations of diagnostic marine boundary layer models applied to hurricanes. *Mon. Wea. Rev.*, **108,** 757–766.

——, 1982: The transition of the Hurricane Frederic boundary-layer wind field from the open Gulf of Mexico to landfall. *Mon. Wea. Rev.*, **110,** 1912–1932.

——, 1990: Boundary layer structure and dynamics in outer hurricane rainbands. Part I: Mesoscale rainfall and kinematic structure. *Mon. Wea. Rev.*, **118,** 891–917.

——, P. P. Dodge, and M. L. Black, 1991: The landfall of Hurricane Hugo in the Carolinas. *Wea. Forecasting,* **6,** 379–399.

Saffir, H. S., 1977: Design and construction requirements for hurricane resistant construction. Preprint No. 2830, American Society of Civil Engineers, 20 pp.

Saffle, R. E., 1976: D/RADEX products and field operation. Preprints, *17th Radar Meteorology Conf.*, Seattle, WA, Amer. Meteor. Soc., 555–559.

Sheets, R. C., 1990: The National Hurricane Center—Past, present, and future. *Wea. Forecasting,* **5,** 185–232.

WAMDI Group (S. Hasselmann, K. Hasselmann, E. Bauer, P. A. E. M. Janssen, G. J. Komen, L. Bertotti, P. Lionello, A. Guillaume, V. C. Cardone, J. A. Greenwood, M. Reistad, L. Zambresky, and J. A. Ewing), 1988: The WAM model—A third generation ocean wave prediction model. *J. Phys. Oceanogr.*, **18,** 1775–1810.

Willoughby, H. E., J. A. Clos, and M. G. Shoreibah, 1982: Concentric eye walls, secondary wind maxima, and the evolution of the hurricane vortex. *J. Atmos. Sci.*, **39,** 395–411.